

A REVIEW OF LAMINAR SINGLE-PHASE FLOW IN MICROCHANNELS

Ian Papautsky
Dept. of Electrical and Computer Engineering
University of Cincinnati

Tim Ameen
Department of Mechanical Engineering
University of Utah

A. Bruno Frazier
School of Electrical and Computer Engineering
Georgia Institute of Technology

ABSTRACT

Microfluidics plays a major role in the development of many innovative research activities aimed at the development of miniaturized devices and systems, and new applications related to microscale handling of fluids. As the field of microfluidics continues to grow, it is becoming increasingly important to understand the mechanisms and fundamental differences involved in microscale fluid flow. This paper presents a summary of the experimental research efforts in the area of microscale single-phase internal fluid flow and discusses issues associated with investigating microscale flows. While the currently available experimental data indicate the presence of microscale phenomena, they do not unequivocally identify the effects. There is a clear need for additional experimental investigations.

INTRODUCTION

Over the past decade, micromachining technology has been used to develop a number of microfluidic systems in silicon, glass, quartz, and plastics. Microchannels and chambers are essential components of any such system. In addition to connecting different devices, microchannels are also used for reactant delivery, as bio/chemical reaction chambers [1,2], in physical particle separation [3-5], in inkjet print heads [6,7], or as heat exchangers for cooling computer chips [8,9]. Currently, fluid flows in microchannels and micromachined fluid systems (e.g., pumps and valves) are analyzed using the Navier-Stokes equations [10,11]. However, a number of publications have shown that (a) flows on the microscale are different from that on the macroscale and that (b) the Navier-Stokes equations alone are incapable of modeling the occurring phenomena [12-14]. Thus, in order to design and fabricate such microdevices effectively, the fluid flow on the microscale must be better understood.

Several effects, which are normally neglected when considering macroscale flow, may be significant on the microscale. The first of these microscale phenomena are the two- and three-dimensional transport effects. As characteristic lengths are reduced to the same order of magnitude as the hydrodynamic boundary layer thickness, momentum transfer in directions other than the streamwise direction can increase significantly [15]. Another observed microscale effect is that of temperature variations in the transport fluid that can cause a significant variation in fluid properties (e.g., apparent fluid viscosity) throughout a microsystem, invalidating the often-used assumption of constant properties [16]. Other effects that may play a more significant role on the microscale include viscosity variation near the solid surface, slip flow at the boundary, and micropolar fluid effects.

Fluid dynamics in general is an empirical science that relies heavily on experimentation to determine the effects of changes in flow parameters. Unfortunately, until recently the ability to fabricate channels for microfluidic testing has been limited. With the advent of micromachining, a completely new realm of techniques for precise fabrication of microscale channels has emerged. The ability to precision fabricate channels, though, has not yet resolved the question regarding microfluidic effects. Whether the difficulty related to data collection and analysis of this type is related to the difficulty in making measurements at dimensions of this size or other factors, the questions regarding scale effects in microchannel fluid flow have not yet been answered satisfactorily. Consequently, much work remains to be completed in this area so that a complete understanding of fluid dynamics in small channels can be realized.

This review paper examines the currently available experimental data for single-phase microscale internal flow and assesses the current state-of-the-art. Since the majority of MEMS and microfluidic applications require fluid flows in the

laminar regime or are limited to the laminar regime due to pressure drop constraints, only laminar data is presented herein. In addition, very little turbulent or transition data is available due to the associated very large pressure drops. Following this introduction, some of the key non-dimensional parameters used herein are defined. In the subsequent section, sources of errors associated with surface effects, measurements of microchannel dimensions, and pressure measurements are suggested. The experimental data for flows of gases and liquids are presented subsequently, while the evaluation of the current state-of-the-art concludes the paper.

NON-DIMENSIONAL PARAMETERS

Two non-dimensional parameters traditionally used to represent fluid flow data are the Reynolds number (Re) and the Darcy friction factor (f). The Reynolds number characterizes the significance of inertial and viscous effects and is defined for all data presented as

$$Re = \frac{\rho u_m D_h}{\mu} \quad (1)$$

where ρ is the fluid density, u_m is the mean fluid velocity, D_h is the hydraulic diameter, and μ is the fluid viscosity. The Darcy friction factor relates friction effects to pressure drop in pipes and ducts, and is given by

$$f = \frac{2D_h \Delta p}{\rho L u_m^2} \quad (2)$$

where L is the pipe length and Δp is the pressure difference. When referring to the Darcy friction factor, it is common practice to present f as a function of Re . The data are also often reported as a normalized friction constant (C^*) vs. Re given as

$$C^* = \frac{(f \cdot Re)_{\text{experimental}}}{(f \cdot Re)_{\text{theoretical}}} \quad (3)$$

where $f \cdot Re$ is dependent on the channel cross-section for laminar flow.

Laminar friction constants for fully developed flow in rectangular channels may be determined analytically for various aspect ratios (α). For all studies considered herein, the aspect ratio has been defined as either height/width or width/height such that $0 \leq \alpha \leq 1$. In determining $f \cdot Re$, theoretical solutions provided by White [17] have been fit with a polynomial equation (with a constant of determination $R^2 = 0.9995$) [18]

$$f \cdot Re = 96(1 - 1.3553\alpha + 1.9467\alpha^2 - 1.7012\alpha^3 + 0.9564\alpha^4). \quad (4)$$

Laminar friction constants for flows through channels or ducts with non-rectangular cross-sections given by Shah and London [19] have also been employed to determine C^* .

Since most of the investigators presented data as C^* vs. Re , data presented in this paper represent a direct translation. The vertical error bars present in some data sets were transferred directly from investigators' papers. In cases where data was presented as volumetric or mass flow rate vs. pressure drop, Re and f were extrapolated. Some investigators presented roughness of their channels as absolute roughness (ϵ_a). In these cases, the relative roughness was calculated as ϵ_a/D_h .

SOURCES OF ERROR IN MICROSCALE FLUID EXPERIMENTS

Fluid experiments that utilize conduits with microscale dimensions have a number of inherent problems that can lead to undetectable errors, undesirable levels of uncertainty, and complications in comparing results to traditional theory and experimental correlations. These experimental difficulties can be categorized into three distinct areas: measurements of channel dimensions, measurements of pressure and flow rate, and surface effects.

Measurements of dimensions

Precise measurement of the cross-sectional dimensions is extremely important in microscale thermal fluid experiments. Friction factor and the laminar friction constant are proportional to D_h^5 and D_h^4 , respectively. Thus, a 5% increase in the hydraulic diameter that is not accounted for in the data reduction can lead to apparent decreases in the friction factor and laminar friction constant of approximately 28% and 22%, respectively. Errors in dimensional measurements may be a result of the measurement technique or due to changes in dimensions that occur under test conditions. Pre-test dimensional measurements are typically used for characterization of the channel. Changes that occur during testing (expansion of the channel under high pressure, for instance) must be taken into account.

Several methods are used for dimensional measurements, including indirect measurement from SEM images and using a surface profilometer or an optical microscope. All of these instruments are typically applied before the channel is completely formed, which indirectly introduces error in addition to the actual measurement uncertainty. For bulk-micromachined channels in silicon or micro-milled microchannels, the depth of the channel is measured and then a top layer is applied to enclose the channel. If the top layer is different from the etched material, the channel is considered to be a hybrid. In many cases, a UV-curable adhesive is employed to bond the two surfaces. The adhesive layer thickness should be added to the channel depth to obtain an accurate assessment of the channel cross sectional area. Under pressure, the channel cross-sectional dimensions may change

due to deformation of the structural material or to compliance of the adhesive.

Surface micromachining, in which a sacrificial layer is used to define inner dimensions of a channel, may also produce dimensional errors. In this technology, measurements of the resist layer are typically assumed to represent the resulting microchannel inside dimensions. Dimensional changes may occur during photoresist removal due to inward wall compliance resulting from strong capillary forces. It is also possible that some residual sacrificial photoresist remains inside the microchannels. Uniformity of the microchannel cross-section can also affect experimental results and can be difficult to precisely control in some microfabrication technologies. Given the strong dependence of the friction factor and laminar friction constant on the microchannel cross-sectional dimensions (or hydraulic diameter) it is imperative that accurate dimensional measurements be made, ideally both pre- and post-test, and that channel compliance be eliminated.

Measurements of pressure and flow rate

Errors introduced through pressure measurements are primarily due to measurement uncertainty of the instruments and to failure to account for entrance and exit effects. Measurement uncertainty can be reduced through proper selection of instrumentation. Elimination of entrance and exit effects is more difficult due to size constraints. Ideally, static pressure should be measured far enough downstream from the entrance so that entrance effects are eliminated. Similarly, the static pressure should be measured upstream of the microchannel exit to eliminate exit effects. In many cases, pressure is measured in manifolds outside the microchannel and the entrance and exit effects have either been estimated or neglected. In other cases, the fluid has been allowed to exhaust to ambient conditions and an assumption of ambient pressure (neglecting pressure drop due to expansion) has been assumed.

Flow rate measurement uncertainty will produce uncertainty in the final test parameters. Proper experiment design and instrument selection can reduce this effect. Instruments capable of low flow rate measurement are usually quite expensive and, therefore, may not be available. An instrument with a higher flow rate range may be used in low flow rate tests if a multi-channel system is fabricated. This type of system requires an assumption of equal flow rates in all of the parallel microchannels. Unfortunately, this assumption introduces another source of error into the experiment.

With the small diameter of the microchannels, in many experiments the flow rate may approach sonic velocity. In these instances, compressibility effects should be accounted for in the data reduction to eliminate another potential error source.

Surface effects

According to laminar fluid theory, friction factor is independent of wall surface roughness. However, on the microscale, molecular interaction with the walls increases relative to intermolecular interaction when compared to

traditional scale flows. Thus, it is unclear if the friction factor is independent of relative roughness on the microscale. Some authors have suggested that the deviations from macroscale theory that have been observed may be due to the large relative roughness of the microchannel walls. Given the uncertainty of the wall roughness effect, the microchannel wall roughness should be characterized in order to complete the data set and to allow each data set to potentially be used to answer this fundamental question.

As mentioned previously, hybrid channels result when microchannels are capped (sealed) with a material other than the substrate material in which the microchannels are etched. These hybrid channels, with two distinct materials and roughness values, make direct comparison of the microchannel data with traditional theory problematic. Some hybrid channels are fabricated by first etching the microchannel pattern in silicon and then sealing the channel with a glass cover plate. These microchannels have a trapezoidal cross section, which complicates the comparison with laminar fluid theory due to the unusual channel profile. In the search for effects that are scale related, it is imperative that the microchannel cross section be characterized accurately in order that comparisons to similar macroscale channels can be accomplished, and that effects due to channel cross-section are eliminated.

SUMMARY OF EXPERIMENTAL DATA

The currently available experimental data is broken into two major groups—one dealing with gases and another with liquids. The gas data are further segregated into flows with slip at the sidewall and non-slip flows. The gases typically used in experiments include nitrogen, argon, helium, and hydrogen. The liquid data are divided into three main groups: water, alcohols (n-propanol and isopropanol), and silicon oil.

Non-slip gas flows

One of the earlier studies of fluid flow on the microscale were performed by Wu and Little [20,21]. They conducted experiments measuring the friction factors for both laminar and turbulent nitrogen and hydrogen gas flows in microchannels to evaluate the performance of Joule-Thompson cryogenic devices. Two types of microchannels were used, with hydraulic diameters ranging from 50 μm to 80 μm . The silicon microchannels were formed by etching in ethylene-diamine-pyrocatechol (EDP) solution, whereas the glass channels were fabricated by an abrasive etching technique similar to sand blasting. The channels were formed using bonding, resulting in one smooth side (glass cover plate) and large relative roughness on the others. Consequently, the surface roughness of these channels varied from smooth, to rough, to abrasive. The widths of the channels were measured using a microscope with a micrometer eyepiece, while the depth was measured using a dial gauge. The minimum scale interval of these measurements was 1 μm . The pressure and flow measurements were taken using macroscale instruments outside the flow microchannel.

The data collected by Wu and Little [20] is for $10^2 \leq Re \leq 10^4$ and is presented in Figure 1. The normalized friction constant for all the data is greater than unity, which, according to Wu and Little, indicates higher friction than predicted by macroscale theory. The glass channels show the greatest deviation from macroscale theory, which is most likely due to roughness effects caused by the fabrication technique. The data showed transition from laminar to turbulent flow to be at approximately $Re = 500$.

Pfahler et al. [16,22,23] and Harley et al. [24,25,26] presented a number of papers on microscale gas flow. The channels tested are approximately 100 μm wide with depths ranging from 0.5 to 50 μm . The majority of the channels tested had a low aspect ratio. The cross-sections of the channels were either trapezoidal or rectangular. The channels were formed by etching <100> and <110> silicon substrates in KOH and subsequently bonding with a glass cover plate.

As previously mentioned, precise knowledge of channel dimensions is extremely important for the accurate evaluation of the flow. However, the earlier papers published by Pfahler et al. [23] and Harley et al. [25] indicate that the cross-sectional dimensions of the small channels were approximate, with depth measurements having $\pm 20\%$ accuracy. In addition, the pressure measurements were taken at the inlet of the test section and not within the microchannel. Thus, the entrance effects were not accounted for. Pressure losses in the fittings were estimated to be a small fraction of the total pressure drop, typically around 2%, while the exit pressure was assumed to be approximately equal to atmospheric pressure [23,25].

In the later studies, the channel dimensions were measured more accurately [16,22,24]. The width of the channels was measured optically using a calibrated microscope reticle at 200 \times . The depth was measured with a surface profilometer within 2% [16,22]. The surface of these latter channels was rough, with relative roughness of approximately 0.01. However, the pressure measurements were still taken outside the channel using external transducers, with pressure losses in the fitting estimated to be approximately 2%. The experimental uncertainties in f and Re were reported to be less than 10%.

Pfahler et al. [16,22,23] and Harley et al. [24-26] tested three gases—nitrogen, helium, and argon. The data for these experiments are also presented in Figure 1. Data presented by Harley at al. [24] for flow of all three gases through the same microchannel is within $\pm 5\%$ of $C^* = 1$ for $10 \leq Re \leq 10^3$. The data for $Re < 500$ are entirely 5% below the theoretical values ($C^* < 0.95$), while the remaining few data points are 5% above ($C^* > 1.05$). This increase in C^* may represent the transition to turbulent flow, which agrees with the studies of Wu and Little [20]. The remaining data by Pfahler et al. [16,22] is for the flow of nitrogen in the range $10^{-2} \leq Re \leq 10^2$ which resulted in $0.8 \leq C^* \leq 0.9$.

Choi et al. [27] conducted experiments on the friction characteristics of nitrogen gas in circular tubes with diameters ranging from 3 to 81 μm . This was the first experimental study

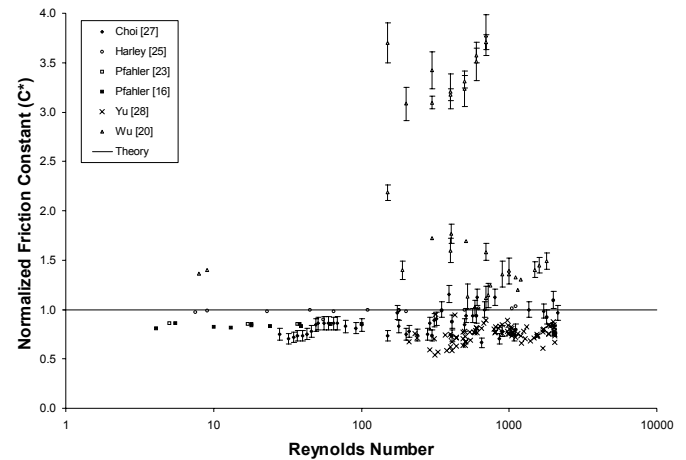


Figure 1. Experimental data for flow of gases.

using microtubes instead of microchannels. Miniature transducers were used to measure pressure and flow. However, these measurements were still taken outside the microtube, thus not accounting for entrance or exit effects. The pressures involved in the experiments were high enough to warrant the use of compressible flow analysis. The friction factor uncertainty was reported to be approximately 13%. Tubes used by Choi et al. [27] were smooth with $0.00017 \leq \epsilon_a/D_h \leq 0.0116$. The data showed the friction factors to be as much as 30% lower than that predicted by theory for flows with $10 \leq Re \leq 500$. For $Re > 500$, friction factor increased by 15%. This is similar to the data presented by Harley et al. [24], and may be due to transition to turbulent flow. In addition, the microtubes that produced $C^* > 1$ had $\epsilon_a/D_h \approx 0.01$, which is similar to the roughness of channels used by Harley et al. [24].

Yu et al. [28] extended the work of Choi et al. [27] by conducting experimental and theoretical studies of flow and heat transfer characteristics in microtubes. Yu et al. [28] determined the friction factors of nitrogen gas in microtubes with diameters ranging from 19 μm to 102 μm . The inside diameter of these microtubes was measured by an SEM at the two ends and no noticeable variation in diameters was found. Relative roughness of the inner surface measured using a laser interferometer was found to be approximately 0.003. The flow rate of nitrogen gas was measured after leaving the test section using an external flowmeter, while two pressure regulators were used to measure the inlet and outlet pressures. Consequently, entrance and exit effects were not accounted for. The Reynolds numbers for the experimental data are in the range of 100 to 1500, while the laminar friction constant is 60% to 90% of the theoretical value of 64. This behavior is consistent with data of Choi et al. [27]. The average friction constant ranged from 49.35 to 51.56, which is somewhat lower than that obtained by Choi et al. ($f-Re \approx 53$) [27].

Overall, the available data (Figure 1) can be divided into two main groups. The first group contains the data that is quite consistently in the $0.8 < C^* < 1$ range. However, uncertainties

associated with channel dimensions and unaccounted or poorly accounted entrance and exit effects prevent one from making a definitive conclusion. The second group of data appears at $Re > 500$ and has a wide range of C^* . The data with very large C^* from Wu and Little [20] were measured in microchannels with rough surfaces. Although no actual roughness values were given, the authors have indicated that the apparent increase in laminar friction constant in their data is probably due to surface roughness effects. It is also possible that we are seeing a transition to turbulence, especially at $Re > 1000$, as it is conceivable that turbulence occurs at lower Re on the microscale. Transition to turbulence would not only explain higher C^* for Wu and Little [20], but also a reduction of C^* to 0.6 for Choi et al. [27] and Yu et al. [28] who verified microtube diameters with SEM. Overall, the experimental measurement uncertainties, possible early transition to turbulence, and potential roughness effects suggest that much more data are needed to form solid conclusions for this type of microscale flow.

Slip gas flows

Arkilic et al. [29,30] investigated helium flow through microchannels for pressure drops of 0.2 to 1.5 atm. The microchannels were 52.25 μm wide, 1.33 μm deep, 7.5 mm long, and were formed by bonding two oxidized silicon wafers. The shape of the channel was determined by etching the silicon dioxide covering one side of one wafer, while the input ports were formed by etching through the other wafer. The absolute roughness of these channels was 65 nm, with a relative roughness of 0.00025. Both flow and pressure measurements were taken externally using macroscale transducers.

The experimental results showed that the pressure drop over the channel length was less than the continuum flow results. In fact, the friction constant was only 35-45% of the theoretical values, as shown in Figure 2. This significant reduction in the friction constant may be due to the slip/transition flow regimes, as the Knudsen number for the data ranges from 0.027 to 0.594. Thus, according to the flow regime classification by Beskok and Karniadakis [31], the flows studied by Arkilic et al. [29,30] are well within the slip flow regime, or in some cases even in the transition flow regime. A model based the Navier-Stokes equations with slip flow boundary condition was able to predict the flow accurately (assuming steady, incompressible, isothermal flow with negligible entrance and exit effects). It must be noted, however, that the experimental results by Arkilic et al. [29,30] were for very low Reynolds number flow, $4 \times 10^{-3} < Re < 0.5$.

Pong et al. [32] investigated helium and nitrogen gas flows through $5 \times 1.2 \times 3000 \mu\text{m}^3$ and $40 \times 1.2 \times 3000 \mu\text{m}^3$ ($W \times H \times L$) microchannels using a microfabricated flow system. Pressure sensors were fabricated as an integral part of the flow channels, allowing measurements of not only the overall pressure drop and flow rate, but also pressure distribution along the microchannel. It was found that the pressure distribution was not a linear function as suggested by a continuum flow

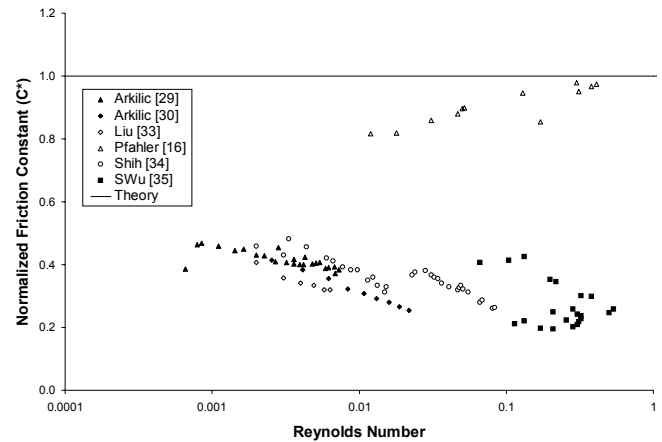


Figure 2. Experimental data for slip flow of gases.

analysis, indicating a lower pressure drop through the channel than predicted for continuum flow. The nonlinear pressure distribution becomes more pronounced as Knudsen number increases. Pong et al. [32] suggested that such non-linearity is due to the compressibility of the fluid and the slip flow effects. The normalized pressure data showed the presence of a large viscous effect.

Liu et al. [33] used the flow system described by Pong et al. [32] to further study microscale gaseous flow. Experimental results were obtained for both uniform and non-uniform cross-section channels. The uniform channel dimensions were $40 \times 1.2 \times 4500 \mu\text{m}^3$ ($W \times H \times L$). The pressure drop distribution was shown to be nonlinear. This is consistent with the results found by Pong et al. [32]. Unfortunately, Liu et al. [33] was unable to find a definite relationship between flow rate and pressure. Due to very low Reynolds numbers in the study ($0.001 < Re < 0.01$), the inertial effects were neglected in the mathematical model. It was found that a steady, isothermal, continuum flow with a slip boundary condition accurately modeled the flow situation. However, the experimental results showed that the pressure gradients near the inlet and outlet were small, which cannot be explained by the model.

Shih et al. [34] furthered the work of Pong et al. [32] and Liu et al. [33] by conducting more detailed fluid flow studies. In addition to measuring the overall pressure drop and flow rate, Shih et al. [34] also measured the pressure distribution along the microchannel. The microchannel used in the study was similar to the one used by Liu et al. [33] previously. The only difference was the reduced channel length, with total dimensions being $40 \times 1.2 \times 4000 \mu\text{m}^3$ ($W \times H \times L$). The reduction in channel length resulted from the fact that two of the integrated pressure sensors closest to the channel ends were not used due to end effects. The total number of pressure sensors along the channel length was eleven.

Shih et al. [34] used two gases for the flow experiments—helium and nitrogen. The Reynolds number range for the flow data is $0.001 < Re < 0.1$, while the friction constant is only 30-45% of the theoretical values ($0.3 < C^* < 0.45$). This

significant reduction in the friction constant is most likely due to the slip/transition flow regimes, as the Knudsen number for the data ranges from 0.02 to 0.16. This friction constant reduction is consistent with the results of Liu et al. [33] and Arkilic et al. [29,30].

Wu et al. [35] investigated fluid flow and frictional heating in microchannels. The microchannels used in this study were 19 μm in width, 1.85 μm in height, and 4.4 mm in length. The channels were surface fabricated using sacrificial phosphosilicate glass (PSG) and silicon nitride as the structural material. In addition, the channels were suspended from the silicon substrate using dry etching for thermal isolation. The inlet pressure was measured using an external pressure transducer, while the exit pressure was measured using a digital manometer. According to the authors, these transducers had an uncertainty of approximately 7 to 0.7 kPa respectively. As the authors point out, however, in order to truly ascertain pressures, it is necessary to integrate pressure transducers immediately at the ends of the microchannel. For nitrogen gas flow, the data are in the $0.1 < Re < 1$ range, while the normalized friction constant is $0.3 < C^* < 0.4$. This reduction in the normalized friction constant is consistent with the results of Liu et al. [33] and Arkilic et al. [29,30].

The slip gas flow data (Figure 2) appear in two groups. The first large group contains the data in the $0.2 < C^* < 0.5$ range indicating an apparent 60% reduction in laminar friction constant due to slip effects. This conclusion is supported by the modeling efforts of Arkilic et al. [29,30] and Liu et al. [33]. The data of Arkilic et al. [29,30], Liu et al. [33], and Shih et al. [34] are the least susceptible to measurement uncertainties. The second small group is the data from Pfahler et al. [16] with $C^* \sim 0.9$. The measurement uncertainty associated with channel dimensions and the failure to account for entrance and exit losses suggest that the data are less likely to accurately portray the slip flow effects.

Water flows

In recent studies, Papautsky et al. [36,37] examined flow of water through arrays of surface micromachined metallic microchannels on top of silicon substrates. These channels had rectangular cross-section with inner width ranging from 150 μm to 600 μm and inner heights varying from 22.71 μm to 26.35 μm . Liquid input ports were etched through the silicon substrate. Additional ports were etched through silicon for static pressure measurements approximately 4.5 mm downstream, which eliminated entrance effects. The open ends of the microchannels extending off the silicon substrate were used as flow outlets. The channel length between the static pressure port and the open end was 7.75 mm. The channel cross-sectional dimensions were measured with a surface profilometer with a precision of 10 nm. Surface roughness of the microchannels was determined to be approximately 0.00033 using atomic force microscopy. The liquid flow was supplied by a controllable syringe pump. The uncertainty analysis showed the average uncertainties in f and Re to be

7.77% and 1.51% respectively at low pressures and 5.61% and 0.13% at high pressures. The experimental data of this study, presented in Figure 3, are for $0.001 < Re < 10$ and shows a 20% increase in the normalized friction constant ($C^* \approx 1.2$) from the theoretical values.

Similar results were obtained by Jiang et al. [38], who investigated flow of water through microchannels, nozzles, and diffusers. Microchannels used in this study had rectangular, trapezoidal, or triangular cross-sections, and were formed by KOH etching a silicon substrate then sealed by bonding it with a glass wafer. The microchannel dimensions ranged from 35 μm to 110 μm in width and from 13.4 μm to 46 μm in height, whereas the lengths varied from 2.5 mm to 10 mm. The authors did not specify roughness of the channel surfaces. Pressure measurements were taken using external pressure transducers, while volumetric flow rates were derived from observations of meniscus position using a microscope and a CCD camera. For the 10 mm long microchannel, Re ranged from 0.1 to 10 and the normalized friction constant is 15-30% above the theoretical values ($1.15 < C^* < 1.3$). For the shorter 5 mm channel with the identical cross-sectional dimensions, the flow data are in the same Re range but have a significantly higher normalized friction constant ($1.5 < C^* < 1.75$). Since channel length is the only difference between the two cases, the increase in the normalized friction constant might be attributed to the entrance effects in the shorter channels.

Gale [39] investigated flow of water through individual microchannels of low aspect ratio. The microchannels fabricated as a part of a biochemical analysis system were formed using an epoxy-like polymer sandwiched between a bottom silicon substrate and a top glass cover. The channel widths ranged from 4 mm to 6 mm while heights varied from 14.5 μm to 50 μm . The channel input ports were etched through the silicon substrates. Additional ports were etched in silicon for static pressure measurements 4.5 mm downstream in order to eliminate entrance and exit effects. The channel length between the static pressure ports was 5 mm. The channel height measurements were performed using a microscope with z -dimension measurement capability with resolution of 1 μm .

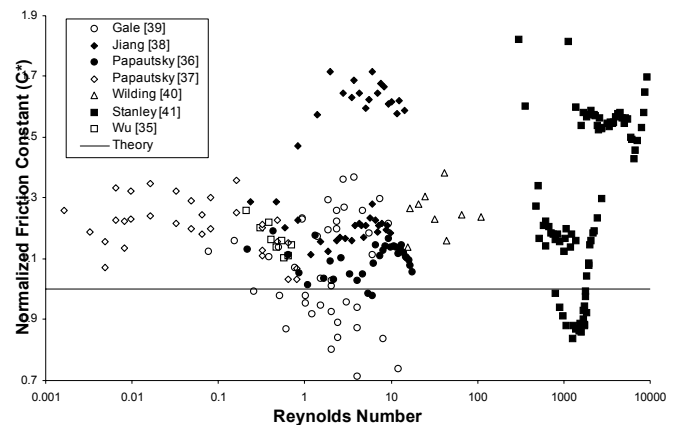


Figure 3. Experimental data for flow of water.

Roughness of the microchannel inner surface was not characterized. A controllable syringe pump supplied the liquid flow. The data collected in this study are for $0.1 < Re < 20$ and is shown in Figure 3. The data appear within $\pm 30\%$ of the theoretical values ($0.7 < C^* < 1.35$). The author suggested that such a large variation in the normalized friction constant is due to variation in channel height along the channel length. It is also possible that wide range in the normalized friction constant is due to the poor measurement of the microchannel height.

Wilding et al. [40] analyzed flow of water and various biological fluids (saline, serum, plasma, and whole blood) in glass-capped silicon microchannels. The channels had trapezoidal cross-section with dimensions of $80 \times 20 \mu\text{m}^2$ (W×H) and $150 \times 40 \mu\text{m}^2$. Entrance and exit ports ($500 \times 500 \mu\text{m}^2$) were etched through the silicon substrate with spacing (i.e. channel length) of 11.7 mm. The channel dimensions were measured with a surface profilometer with a precision of $\pm 1\%$. The authors did not specify roughness of the microchannels. The liquid flow was supplied by connecting the inlet port to a syringe whose plunger was actuated by a stepper motor. A load cell measured the applied force from which the driving pressure was deduced. The force measurement was corrected for frictional losses in the system. The authors estimated the pressure losses in the syringe and supply piping to be less than 1% of the total pressure drop. The experimental data of this study, shown in Figure 3, are for $10 < Re < 100$ and indicate a 30% increase in the normalized friction constant ($C^* \approx 1.3$) from the theoretical values.

Stanley [41] studied single-phase and two-phase flows in arrays of rectangular microchannels. Experiments were conducted using rectangular channels formed by precision machining of aluminum substrates that were then covered with glass plates. A UV-curable adhesive was used for sealing. The hydraulic diameters of these channels ranged between 56 and 256 μm , while the aspect ratios varied from 0.5 to 1.5. The input and output ports were formed by drilling through holes in the bottom of the aluminum substrate. The pressure drop measurements were taken immediately outside the microchannel access ports. The single-phase tests were performed using water. Relative roughness of the microchannels varied from 0.0004 to 0.016. The experimental data, shown in Figure 3, are in the $100 < Re < 10000$ range and show the normalized friction constant varying from 20% below to up to 90% above the theoretical values ($0.8 < C^* < 1.9$). A few additional data sets (not shown in Figure 3) appear at approximately 200-300% above theory. These data sets are for the microchannels with surface roughness above 0.002, indicating that such a significant increase in the normalized friction constant may be due to the roughness of the microchannel walls. Stanley [41] data appear over a wide range of C^* with $Re \approx 1000$, which may indicate a possible onset of turbulence. However, the pattern of the data is not at all consistent with what might be expected if transition is considered.

As mentioned earlier, Wu et al. [35] investigated flows of water and nitrogen gas in microchannels. The surface micromachined channels were 19 μm in width, 1.85 μm in height, and 4.4 mm in length. The volumetric flow rate in experiments using water was measured optically using the position of a water meniscus over time. The water flow data are in the narrow Reynolds number range, $0.1 < Re < 1$. The values of the normalized friction constant are 10-30% above the theoretical values ($1.1 < C^* < 1.3$), which is consistent with the results of Wilding et al. [40] and Jiang et al. [38].

Overall, it appears that there may be an approximately 20% increase in laminar friction constant as the majority of data are in the $1.1 < C^* < 1.3$ range. Entrance effects and transition to turbulence might explain Jiang et al. [38] and Stanley [41] data that have higher normalized friction constant values ($C^* > 1.3$). More data are needed before unequivocal conclusions can be reached.

Alcohol flows

Pfahler et al. [16,22,23] and Harley et al. [24-26] presented a number of papers on microscale flow of alcohols. The channels tested were approximately 100 μm wide with depths ranging from 0.5 to 50 μm . The majority of the channels tested had a low aspect ratio. The cross-sections of the channels were either trapezoidal or rectangular. The channels were formed by etching $\langle 100 \rangle$ and $\langle 110 \rangle$ silicon substrates in KOH and subsequently bonding with a glass cover plate.

The experimental data for flow of alcohols, shown in Figure 4, have $0.8 \leq C^* \leq 1$. Very few data sets are outside this range. The data sets in the range of three to four times the normalized friction constant belong to the earlier studies with less accurate channel dimensions. While surface roughness may have an effect, similar to the effects seen in the Wu and Little [20,21] data, these discrepancies are most likely due to the uncertainty in the channel dimensions. Overall, Re range is quite wide, spanning seven orders of magnitudes between approximately 10^{-4} and 10^3 . While it appears that there is a

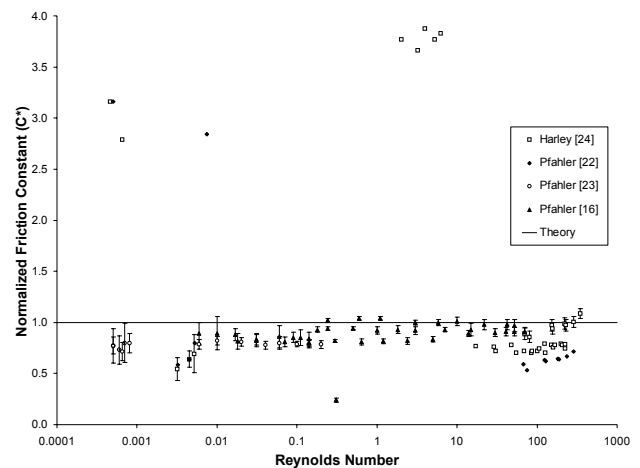


Figure 4. Experimental data for flow of alcohols.

20% decrease in laminar friction constant, the lack of supporting studies by other investigators suggests that more work is needed before conclusions regarding microscale effects can be drawn.

Silicon oil flows

Pfahler et al. [16,22,23] and Harley et al. [24-26] collected the experimental data for flow of silicon oil using the microchannels from the studies of alcohol flows. The silicon oil data are presented in Figure 5. The data for $Re > 0.1$ are approximately 85% of the theoretical values. The data sets at $Re \approx 0.01$ that are 70-80% of theoretical values belong to the earlier studies. Although Figure 5 suggests a Re dependence for silicon oil flows in microchannels, the 25-30% deviation of the data from the theoretical values at low Re may be due to the uncertainty of the microchannel dimensions. The narrow Re range and lack of supporting studies by other researchers strongly suggest that more work is needed for this class of fluids. No conclusions regarding microscale effects can be made.

CONCLUSIONS

A comprehensive study of the results of microscale single-phase internal flows has been compiled. The only definitive conclusion that can be reached from the currently available data is that *slip flow gas data indicate an approximate 60% reduction in f compared to macroscale theory at the same Re .* The currently available experimental data for other types of flows are inconclusive as they appear both above and below the theoretical predictions (although data for each researcher are consistently either greater or less than theoretical values). In part, these results may be attributed to roughness of the channels and to uncertainty in the determination of channel dimensions. Part of the discrepancy may also be due to the lack of a well-controlled surface structure, as the bonding of silicon and glass is the predominant method for microchannel fabrication. In addition, while some researchers estimate the entrance effects, to truly ascertain the microchannel friction factor, the measurements must be taken within the microchannel near the channel entrance and exit. The preliminary conclusions that can be made regarding non-slip fluid flows are:

1. Microchannel surface roughness appears to increase f , which seems to intensify with higher surface roughness;
2. Laminar friction constant appears to be approximately 20% higher than the theoretical predictions for flow of water;
3. No reliable range of Re for turbulence transition has been reported; some data seems to suggest that turbulence occurs at lower Re values on the microscale (as low as $Re = 500$);

The overall conclusion is that *while the currently available experimental data suggest the presence of microscale*

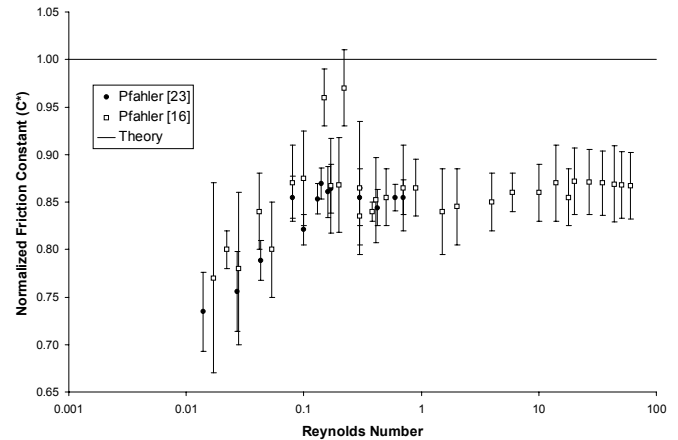


Figure 5. Experimental data for flow of silicone oil.

phenomena, they do not unequivocally identify the effects. There is a clear need for additional experimental investigations over a wider Re range using microchannels with well-characterized dimensions and surface roughness and well-designed experimental methods in order to understand microscale single-phase internal fluid flow. At present, *accurate* prediction of pressure drops in microchannels for non-slip flows is not possible, although *estimates* of pressure drops can be made using the traditional theory and correlations.

REFERENCES

1. Srinivasan, R., Hsing, I.-M., Ryley, J. Harold, M. P., Jensen, K. F., and Schmidt, M. A., 1996, "Micromachined chemical reactors for surface catalyzed oxidation reactions," IEEE Solid-State Sensor and Actuator Workshop, Hilton Head, SC, June 2-6.
2. Van Den Berg, A., Olthuis, W., and Bergveld, P., eds., 2000, Micro Total Analysis Systems 2000, Kluwer Academic Publishers, Boston, MA.
3. Reston R. and Kolesar, E., 1994, "Silicon-micromachined gas chromatography system used to separate and detect ammonia and nitrogen dioxide," *J. Microelectromech. Sys.*, vol. 3, pp. 134-146.
4. Effenhauser, C., Manz, A., and Widmer, M., 1993, "Glass chips for high-speed capillary electrophoresis separation with submicrometer plate heights," *Anal. Chem.*, vol. 65, pp. 2637-2642.
5. Harrison, D. J., Fan, Z., Fluri, K., and Seiler, K., 1994, "Integrated electrophoresis systems for biochemical analysis," IEEE Solid-State Sensor and Actuator Workshop, Hilton Head, SC, June 13-16.
6. Allen, R., Meyer, J., and Knight, W., 1985, "Thermodynamics and hydrodynamics of thermal ink jets," *Hewlett-Packard Journal*, vol. 36, no. 5, pp. 21-27.
7. Krause, P., Obermeier, E., and Wehl, W., 1995, "Backshooter—A new smart micromachined single-chip

- inkjet printhead," *Transducers '95*, Stockholm, Sweden, June 25-29, pp. 325-328.
8. Bowers, M. B. and Mudawar, I., 1994, "Two-phase electronic cooling using mini-channel and micro-channel heat sinks," *Trans. ASME*, vol. 116, p. 290.
 9. Tuckerman, D. B. and Pease, R. F. W., 1981, "High-performance heat sinking for VLSI," *IEEE Electron Dev. Lett.*, vol. EDL-2, No. 5, pp. 126-129.
 10. Brody J. and Yager, P., 1996, "Low Reynolds number micro-fluidic devices," Solid-State Sensor and Actuator Workshop, Hilton Head, SC, June 2-6, pp. 105-108.
 11. Jiang, X. N., Zhou, Z. Y., Yao, J., Li, Y. and Ye, X., 1995, "Micro-fluid flow in microchannel," *Transducers '95*, Stockholm, Sweden, June 25-29, pp. 317-320.
 12. Peng, X. F., and Wang, B. X., 1994, Proc. 10th International Heat Transfer Conference, Brighton, UK, Aug. 14-18, pp. 159-177.
 13. Holmes, D. B., and Vermeulen, J. R., 1968, *Chem. Engng. Sci.*, Vol. 23, pp. 717-722.
 14. Migoun, N., 1996, *Kapilarna wiskozymetria dla mikroobjemow zydkostej*, Sankt Petersburg, Russia.
 15. Ma, S. W., and Gerner, F. M., 1993, "Forced convection heat transfer from microstructures," *J. Heat Transfer*, vol. 115, pp. 872-880.
 16. Pfahler, J., Harley, J., Bau, H., and Zemel, J. N., 1991, "Gas and liquid flow in small channels," ASME Micromechanical Sensors, Actuators, and Systems, vol. DSC-32, pp. 49-60.
 17. White, F. M., 1994, *Fluid Mechanics*, 3rd ed, McGraw Hill, New York, NY.
 18. Hartnett, J. P., and Kostic, M., 1989, "Heat transfer to Newtonian and non-Newtonian fluids in rectangular ducts," *Advances in Heat Transfer*, vol. 19, pp. 247-356.
 19. Shah, R. K., and London, A. L., 1978, *Laminar Flow Forced Convection in Ducts*, Academic Press, New York.
 20. Wu, P., and Little, W. A., 1983, "Measurement of friction factors for the flow of gases in very fine channels used for microminiature joule-thomson refrigerators," *Cryogenics*, no. 5, pp. 273-277.
 21. Wu, P., and Little, W. A., 1984, "Measurement of the heat transfer characteristics of gas flow in fine channel heat exchangers used for microminiature refrigerators," *Cryogenics*, no. 8, pp. 415-419.
 22. Pfahler, J., Harley, J., Bau, H., and Zemel, J., 1990, "Gas and liquid transport in small channels," ASME Microstructures, Sensors, and Actuators, vol. 19, pp. 149-157.
 23. Pfahler, J., Harley, J., and Bau, H., 1990, "Liquid transport in micron and submicron channels," *Sensors and Actuators*, vol. A21-23, pp. 431-434.
 24. Harley, J., Huang, Y., Bau, H., and Zemel, J. N., 1995, "Gas flow in micro-channels," *J. Fluid. Mech.*, vol. 284, pp. 257-274.
 25. Harley, J., Pfahler, J., Bau, H., and Zemel, J. N., 1989, "Transport processes in micron and submicron channels," *ASME Heat Transport Processes*, vol. HTD-116, pp. 1-5.
 26. Harley, J., Bau, H., Zemel, J. N., and Dominko, V., 1989, "Fluid flow in micron and submicron size channels," MEMS '89, Salt Lake City, UT, Feb. 20-22, pp. 25-28.
 27. Choi, S., Barron, R., and Warrington, R., 1991, "Fluid flow and heat transfer in microtubes," ASME Micromechanical Sensors, Actuators, and Systems, vol. 32, pp. 123-134.
 28. Yu, D., Warrington, R. O., Barron, R., and Ameel, T., 1995, "An experimental and theoretical investigation of fluid flow and heat transfer in microtubes," ASME/JSME Thermal Engineering Conf., March, Maui, Hawaii.
 29. Arkilic, E. R., Breuer, K. S., and Schmidt, M. A., 1994, "Gaseous flow in microchannels," ASME Appl. Microfab. Fluid Mech., vol. FED-197, pp. 57-66.
 30. Arkilic, E. R., Schmidt, M. A., and Breuer, K. S., 1997, "Gaseous slip flow in long microchannels," *IEEE J. Microelectromech. Sys.*, vol. 6, no. 2, pp. 167-178.
 31. Beskok, A., and Karniadakis, G. E., 1992, "Simulation of slip-flows in complex micro-geometries," *Proc. ASME*, vol. DSC-40, pp. 355-370.
 32. Pong, K., Ho, C., Liu, J., and Tai, Y., 1994, "Non-linear pressure distribution in uniform microchannels," ASME Applications of Microfabrication to Fluid Mechanics, vol. FED-1997, pp. 51-56.
 33. Liu, J., Tai, Y.-C., and Ho, C.-M., 1995, "MEMS for pressure distribution studies of gaseous flows in microchannels," Amsterdam, The Netherlands, Jan. 29-Feb. 2, pp. 209-215.
 34. Shih, J. C., Ho, C., Liu, J., and Tai, Y., 1996, "Monatomic and polyatomic gas flow through uniform microchannels," ASME MEMS, vol. DSC-59, pp. 197-203.
 35. Wu, S., Mai, J., Zohar, Y., Tai, Y., and Ho, C., 1998, "A suspended microchannel with integrated temperature sensors for high pressure flow studies," MEMS '98, Heidelberg, Germany, Jan. 25-29, pp. 87-92.
 36. Papautsky, I., Brazzle, J., Ameel, T., and Frazier, A. B., 1999, "Laminar fluid behavior in microchannels using micropolar fluid theory," *Sensors and Actuators A*, vol. 73, no.2, pp. 101-108.
 37. Papautsky, I., 1999, "Metallic microinstrumentation for biomedical fluid applications," Ph.D. thesis, University of Utah, Salt Lake City, UT.
 38. Jiang X. N., Zhou, Z. Y., Yao, J., Li, Y., and Ye, X. Y., 1995, "Micro-fluid flow in microchannel," *Transducers '95*, Stockholm, Sweden, June 25-29, pp. 317-320.
 39. Gale, B. K., 2000, "Scaling effects in a microfabricated electric field flow fractionation system with integrated detector," Ph.D. thesis, University of Utah, Salt Lake City.
 40. Wilding, P., Shoffner, M. A., and Kircka, L. J., 1994, "Manipulation and flow of biological fluids in straight channels micromachined in silicon," *Clin. Chem*, vol. 40, pp. 1815-1818.
 41. Stanley, R. S., 1997, "Two-phase flow in microchannels," Ph.D. thesis, Louisiana Tech University, Ruston, LA.